Pulsatile operation of the BiVACOR TAH – Motor design, control and hemodynamics

Matthias Kleinheyer[a], Daniel L. Timms[a,b], Nicholas A. Greatrex[a], Toru Masuzawa[c], O. Howard Frazier[a], William E. Cohn[a]

***Abstract*—Although there is limited consensus about the strict requirement to deliver pulsatile perfusion to the human circulatory system, speed modulation of rotary blood pumps is an approach that may capture the benefits of both positive displacement and continuous flow blood pumps. In the current stage of development of the BiVACOR Total Artificial Heart emphasis is placed on providing pulsatile outflow from the pump. Multiple pulsatile speed profiles have been applied in preliminary in-vivo operation in order to assess the capability of the TAH to recreate a physiologic pulse. This paper provides an overview about recent research towards pulsatile BiVACOR operation with special emphasis on motor and control requirements and developments.**

I. Introduction

The long-term impact of continuous flow perfusion and the necessity of the physiologic pulse has become a critically discussed topic among clinicians and engineers developing state-of-the-art third generation rotary Ventricular Assist Devices (VADs) and Total Artificial Hearts (TAHs)[1]. A compromise between positive displacement type and continuous flow blood pumps is given by the possibility of pulsatile operation of rotary blood pumps. This can be achieved by pump speed modulations, which periodically vary the pump output in an attempt to replicate the natural pulse of the human heart. Different in-vitro and in-vivo studies have been performed during VAD support [2] as well as TAH[3] and Cardiopulmonary Bypass (CPB) operation[4].

Even though promising results were achieved in the past, the potential benefits are controversial. While some studies found the applied pulsatile waveforms not to affect the physiology at all[5], several research groups presented indications that pulsatile perfusion in long-term applications is beneficial[6-8] and can help to ensure sufficient device washout preventing blood clot formation[9]. These discrepancies may be caused by the inconsistent classification of a physiological pulse and potentially inadequate pulsatile pump performance leading to false conclusions[10]. Different metrics to compare pulsatile waveforms are used in different studies[11, 12], which makes a comparison and assessment inaccurate and difficult.

The objective of the study described in this paper is the development of the technical basis for precise generation of pulsatile speed profiles with the BiVACOR Total Artificial Heart, in order to investigate and compare their effects on the circulatory system.

[a] Texas Heart Institute, 6770 Bertner Avenue, Houston, TX, 77030 USA
[b] BiVACOR Inc., Houston, TX, 77004 USA
[c] Ibaraki University, 4-12-1 Nakanarusawa, Hitachi, Ibaraki, JAPAN

II. Quantification of Pulsatile Hemodynamics

Different potential benefits of pulsatile perfusion have been presented. In many approaches researchers tried to measure pulsatile perfusion with a single quantity or recommended a standardized measure, which is certainly advisable in terms of appropriate comparability within different studies and to continuous flow perfusion. However, since multiple aspects have to be taken into account, a single generalized measure evidently capturing all characteristic attributes of the hemodynamic waveforms does not exist. While sufficient end-organ perfusion may be accomplished with a high induced energy gradient measured in terms of energy equivalent pressure[11], baroreceptor response was reported at some extent to be improved with aortic high pressure slopes[7]. Without any claim to completeness, Table 1 summarizes quantities that have mostly been used in literature and that are used in this study.

III. BiVACOR Motor Development

The drive of the BiVACOR Total Artificial Heart (Fig. 2) is an axial flux brushless direct current motor. The stator core contains twelve teeth mounted on the ring-shaped yoke and accommodates the double-layer tooth-coil winding providing the axially directed stator flux. The core is manufactured from compressed iron powder compound to minimize eddy current losses in the teeth and yoke. The opposing rotor is integrated in the levitated pump impeller. Since the left pump cavity and impeller vanes are located in the space between stator and rotor, large magnetic gap lengths of up to 3.8mm apply during pump operation. In order to achieve sufficient efficiency and electromagnetic torque especially for large gaps, ten high energy density *NiFeB* permanent magnets provide the rotor excitation and

Table 1 – Frequently used measures for quantification of pulsatile hemodynamics. PP, pulse pressure; PI, pulsatility index; EEP, energy equivalent pressure; SHE, surplus hemodynamic energy; AOP, aortic pressure; Q_L, systemic flow rate.

Quantity	ID	Formula
Maximum pressure slope[7, 13]	*dP/dt*	$\left(\frac{d}{dt}AOP\right)_{max}$
Pulse Pressure	*PP*	$AOP_{max} - AOP_{min}$
Pulsatility Index	*PI*	$\frac{\int AOP \cdot Q_L \, dt}{\int Q_L \, dt}$
Energy Equivalent Pressure[11, 14]	*EEP*	$\frac{\int P \cdot Q_L \, dt}{\int Q_L \, dt}$
Surplus Hemodynamic Energy[11]	*SHE*	$1332 \cdot (EEP - \overline{AOP})$

are mounted onto the ring-shaped iron yoke which is embedded into the titanium rotor. This is accompanied by a large attractive force to the stator core, which is balanced by the hybrid active and passive magnetic bearing located on the opposing axial side of the pump impeller. The active magnetic bearing is operated with a zero-power control algorithm balancing the impeller in the center of gravity in the unstable magnetic force equilibrium[15]. Due to additional hydraulic forces on the impeller in varying operating points, the center of gravity (i.e. the impeller) moves axially and adjusts the efficiencies of the left and right pump reciprocally by decreasing or respectively increasing the gap between the impeller vanes and the pump housing. This results in adjusted output of both pumps balancing the systemic and pulmonary flows respectively.

A. Design Criteria

In order to achieve the ability to maximize the range of hemodynamic load conditions for which left and right outflow can be automatically balanced, steep hydraulic pressure gradients in combination with low axial magnetic force characteristics for rotor axial movement are desired. This implies the need for a low motor attractive force characteristic, which is mainly determined by the shape and thickness of the permanent magnet and the pole face of the stator core.

Pulsatile operation of the rotary TAH requires a highly dynamic control to generate and compare different rotor speed patterns regarding the resulting hemodynamic pump output waveforms. Since high aortic pressure slopes appear to be a valuable attribute in terms of baroreceptor activation, high accelerating torque and fast control are desired in order to allow quick acceleration of the blood flow. In this regard, the latest iteration of the BiVACOR drive has been designed to achieve the highest torque characteristics for the whole impeller movement range in order to allow high mechanical power output and accurate speed tracking.

B. Geometry optimization

By means of FEM simulations, the geometric dimensions of the stator slots have been varied in order to minimize the design with optimal efficiency within the current and voltage limits determined by the power electronics unit. Three different stators with tooth heights (TH) of 6.5,9.0 and 13mm have been simulated and evaluated regarding back-EMF voltage, torque constant, efficiency and axial attractive force for different slot width (SW) between 4 and 8mm (Fig. 2b).

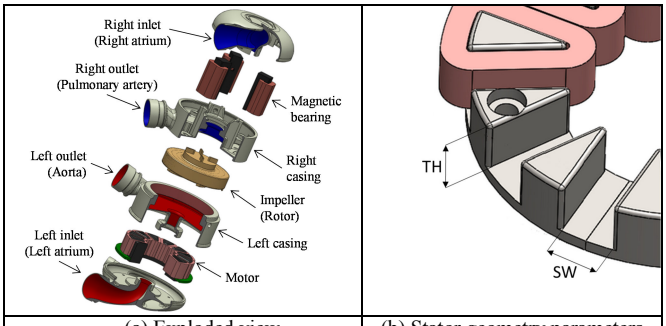

(a) Exploded view (b) Stator geometry parameters

Fig. 2. BiVACOR TAH.

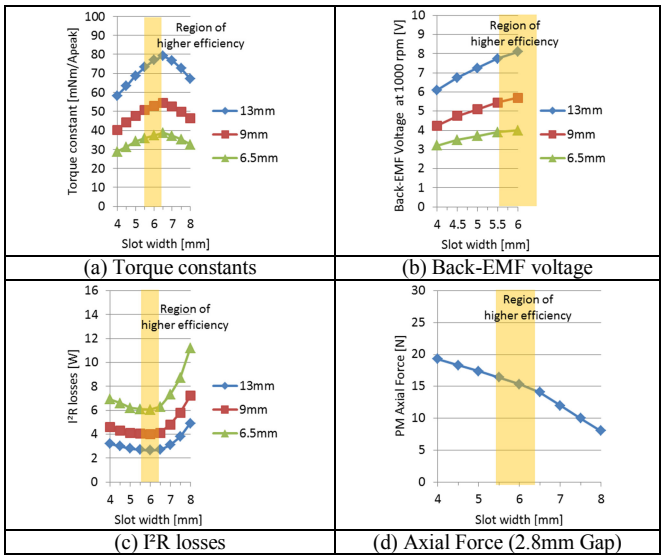

(a) Torque constants (b) Back-EMF voltage

(c) I²R losses (d) Axial Force (2.8mm Gap)

Fig. 1. FEM simulation results for slot width variation. Results are shown for motor models with tooth heights of 6.5, 9 and 13mm.

Fig. 1 shows a comparison of different motor characteristics. The simulated torque constants for different slot widths for motors with the three evaluated stator tooth heights are shown in Fig. 1a. The results indicated that the smallest variant (TH6.5mm) will provide up to 150mNm within the limits of the used power electronics, while significantly decreasing the induced back-EMF voltage (Fig. 1b), size and weight. The motor torque was considered sufficient for the maximum hydraulic load of 100mNm, which has been determined experimentally. Fig. 1c shows the predicted I^2R losses, which showed an optimum region for SW between 5mm and 6.4mm. As expected, the axial attractive force is decreasing towards bigger SW, as the pole-face area of the stator teeth is decreasing (Fig. 1d). However, since the pole-face area is unchanged, no significant change in the axial force for different TH was expected. Since torque constants for all three models strictly increased for SW up to 6.5mm, best efficiency was expected for 6.4mm. Back EMF constants for the TH13mm and TH9mm stator exceeded 8V/1000rpm and 5.5V/1000rpm respectively, indicating that maximum speeds will be limited to less than 4000rpm for operation with supply voltages between 24 and 32V. The copper losses showed a nonlinear increasing trend with TH resulting in decreased efficiency for the smaller variants with TH9mm and TH6.5mm. However, efficiency was sacrificed for the advantage of decreased size, weight and axial force stiffness, which is why the smallest stator variant was chosen. Two prototypes with SW4mm and SW6.4mm were built and compared to the original motor with TH13mm and SW4mm.

In a next optimization step a different motor slot/pole configuration was evaluated. Since the stator core geometry does not need to be varied, the addition of two magnet poles to the rotor allows the realization of a 12-slot/10-pole configuration with a changed stator coil wiring. In contrary to the original motor, the 12/10 winding generates its main torque in the 5th order harmonic instead of the fundamental component of the magnetic gap flux density[16]. This results

in higher torque generation and efficiency, however higher cogging torque was observed which can cause disturbance on the magnetic levitation system. Additionally, higher axial attraction forces were expected due to the additional permanent magnet poles. Three prototypes with different TH/SW combinations (13/4mm; 6.5/4mm; 6.5/6.4mm) were evaluated in a motor test rig and compared to the original 12-slot/8-pole configuration.

C. Speed Control

Hall-effect sensor based six step commutation was initially used for controlling speed however this was replaced by a microcontroller implemented sensorless field oriented control algorithm to improve performance and reliability. The rotational angle was estimated by a sliding mode current observer. A speed and load dependent offset angle was added to eliminate stationary errors. The stator voltages are applied by a three-phase voltage source inverter operated with space vector modulation. Since the motor load conditions change substantially during pulsatile pump operation, the PID speed controller is supplemented by a model-based predictive control to support fast speed tracking. Relative weighting of the model output may allow adaptive adjustment to slow load changes due to varying systemic and pulmonary vascular resistance (SVR/PVR) in the future.

The field oriented control strategy allows active braking control in order to decelerate the impeller[17]. Results by Khalil et al. indicated that pulsatile hemodynamic TAH output showed its maximum at low beat rates, where systemic flow and aortic pressure were allowed to settle to their steady-state minimum values[3]. However, fast impeller deceleration will withdraw hemodynamic energy resulting in faster pump flow deceleration and may hence prevent the observed effect. During the braking cycles the motor is in generator operation allowing energy recovery. This suggests the conduction of future studies regarding the recoverable amount of energy thus reducing the additional power requirements for pulsatile pump operation.

IV. Results

A. In-vivo pulsatile operation

During a preliminary BiVACOR in-vivo study, pulsatile operation tests were performed in order to collect baseline data and evaluate the pump performance for the development of a speed profile resulting in physiologic hemodynamic output. Different speed profiles were applied in order to observe the effects on commonly used metrics for pulsatility. This included slight alterations to the profile, as foregone in-vitro trials suggested their potential big impact on pulsatility. The study was performed in a 6 month old 87.3kg male corriente-cross calf. Fig. 3 shows the results for two slightly different speed profiles, which have been applied within a time-frame of thirty seconds while the calf was resting. The first applied profile (P1) was a square wave profile with an alternation rate of 30bpm and a duty cycle of 50%. Upper and lower set speed levels were defined at 2300 and 2900rpm, correlating to a mean set speed of 2600rpm with an amplitude of 300rpm at an expense of 3.4W additional motor power compared to constant speed operation. The second profile (P2) was slightly altered from P1 by adding an additional spike of 250rpm to the positive half wave, which was exponentially decreasing and ceased after approximately 0.8s during the positive half wave. This resulted in a prolonged acceleration slope in relation to profile P1. The computed resulting mean pump speeds were 2599rpm for the simple square profile P1 and 2631rpm for the extended profile P2. The computed output quantities are summarized in Table 1. The last row shows the perceptual increase of each quantity from P1 to P2.

Table 2 – Summary of pulsatility quantities. dp/dt, maximum pressure slope; MAP , mean aortic pressure; P_M, mean motor power consumption; P_{hyd}, mean hydraulic output power; PP , pulse pressure; EEP , energy equivalent pressure; SHE , surplus hemodynamic energy.

Qty.	dp/dt	MAP	P_M	P_{hyd}	PP	EEP	SHE
Unit	*mmHg/s*	*mmHg*	*W*	*W*	*mmHg*	*mmHg*	*ergs/cm³*
CF	-	106.03	19.45	1.37	-	106.03	-
P1	240.74	101.8	22.86	1.38	24.01	103.43	2064.7
P2	282.71	105.7	23.83	1.43	25.16	107.73	2614.7
% ↑	17.43	3.83	4.24	3.62	4.79	4.16	26.64

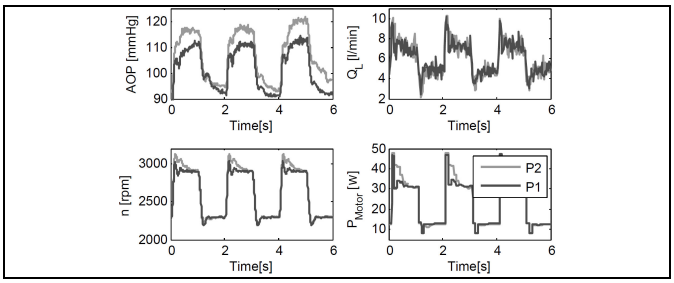

Fig. 3. In-vivo pulsatile results showing aortic pressure (AOP), systemic flow rate (Q_L), motor speed (n) and motor electrical power consumption (P_{Motor}) for two speed profiles P1,P2.

B. Motor evaluation

Fig. 4 shows a summary of the results for five different motor prototypes, which were evaluated in a specifically designed hydraulic and motor test bench. The rotor is attached to a shaft, which is driving an electrically controlled hysteresis brake (Placid Industries H11). Load torque and axial force are measured with a six-axis force/torque sensor (ATI Industrial Automation Mini40-E Transducer) attached to the rotor mounting and used to close a digital control loop, which allows dynamic pump load simulation. Steady-state efficiency measurements were performed for load-torques from 20 – 80mNm at rotor speeds of 500-4000rpm. Axial force stiffness measurements were performed with idle rotor and averaged over the operational magnetic gap range between 2.65 and 3.35mm divided in 0.1mm steps.

V. Discussion

A. Hemodynamics

The results show that considerable pulsatile hemodynamic output can be produced by the BiVACOR TAH with a relatively low target speed wave amplitude of 300rpm. In this first evaluation the pulsatile output is below physiologic waveforms. EEP was observed to exceed MAP by between 1% and 2% for the BiVACOR output waveforms, while physiologic EEP is approximately 10% higher than MAP[13]. However, dP/dt levels with more than 280

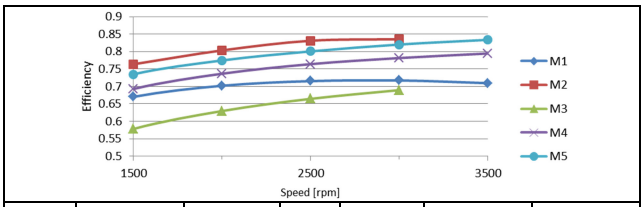

No.	h_t[mm]	w_s[mm]	2p	η_{max}	$\frac{dF}{dx}\left[\frac{N}{mm}\right]$	m[g]
M1	13	4.0	8	0.723	9.15	190
M2	13	4.0	10	0.857	10.49	190
M3	6.5	4.0	8	0.711	7.59	96
M4	6.5	6.4	8	0.803	6.3	103
M5	6.5	6.4	10	0.845	7.16	103

Fig. 4. Prototype evaluation. h_t, tooth height; w_s, slot width; 2p, pole number; η_{max}, maximum efficiency; $\frac{dF}{dx}$, force stiffness; m, stator mass.

mmHg/s were approaching physiologic values (440 – 1180 mmHg/s [10]).

As can be observed from Table 1 all quantities increased when profile P2 was applied. The effect of this relatively slight alteration appears significant and shows that precise speed control is mandatory when pulsatility is compared for different patterns. Control errors like speed overshoot or a slow controller response due to varying load conditions can significantly influence the hemodynamic response.

However, this also suggests that, with an optimized speed profile differing from simple waveforms as square or sine waves, the BiVACOR TAH is capable of generating physiologic hemodynamics.

B. *Improved Drive*

The motor efficiency optimization procedure resulted in a next iteration prototype of the motor drive (M5). Tooth height, slot width and rotor pole number have been changed and resulted in increased efficiency from 72.3% to up to 84.5%. The averaged axial force stiffness was reduced from 9.15 to 7.16 N/mm. The weight of the assembled stator was reduced by 46% compared to the last motor iteration. The improved torque characteristic in combination with a new controller design allows fast and accurate tracking of the defined speed profile.

However, further optimization steps of motor geometry and control are required. Variation of permanent magnet size and shape can be performed in order to achieve sinusoidal back-EMF shape and reduce the weight of the rotor to assist rotational acceleration. In addition, an algorithm based optimization may allow further improvements regarding a specified objective function in order to achieve maximum efficiency operation within the whole operational range of the power electronics inverter. Finally the rotor angle estimator can be improved to ensure maximum torque generation during speed transients.

VI. CONCLUSION

Geometrical and control parameters of the BiVACOR rotary TAH axial flux motor drive were successfully optimized to produce significant pulsatile outflow (86/115mmHg) during speed modulated operation at 30 BPM in an in-vivo animal study. The maximum motor torque of 150mNm produced a significant dP/dt of 280mmHg/s, whilst efficiency was increased to 70-85%. The developed motor may be able to deliver a sufficient physiological pulse to the circulation if required.

REFERENCES

[1] A. UNDAR, "FUNDAMENTALS OF PULSATILE VERSUS NONPULSATILE FLOW DURING CHRONIC SUPPORT," *ASAIO J,* VOL. 49, PP. 139-140, 2003.

[2] R. AMACHER, *ET AL.*, "SYNCHRONIZED PULSATILE SPEED CONTROL OF TURBODYNAMIC LEFT VENTRICULAR ASSIST DEVICES: REVIEW AND PROSPECTS," *ARTIFICIAL ORGANS,* 2014.

[3] H. A. KHALIL, *ET AL.*, "INDUCED PULSATION OF A CONTINUOUS-FLOW TOTAL ARTIFICIAL HEART IN A MOCK CIRCULATORY SYSTEM," *THE JOURNAL OF HEART AND LUNG TRANSPLANTATION,* VOL. 29, PP. 568 - 573, 2010.

[4] A. ÜNDAR, *ET AL.*, "EFFECTS OF PULSATILE VERSUS NONPULSATILE FLOW ON CEREBRAL HEMODYNAMICS DURING PEDIATRIC CARDIOPULMONARY BYPASS WITH DEEP HYPOTHERMIC CIRCULATORY ARREST," IN *ENGINEERING IN MEDICINE AND BIOLOGY SOCIETY*, ISTANBUL, 2001, PP. 480-483, VOL.1.

[5] B. VOSS, *ET AL.*, "CARDIOPULMONARY BYPASS WITH PHYSIOLOGICAL FLOW AND PRESSURE CURVES: PULSE IS UNNECESSARY!," *EUROPEAN JOURNAL OF CARDIO-THORACIC SURGERY : OFFICIAL JOURNAL OF THE EUROPEAN ASSOCIATION FOR CARDIO-THORACIC SURGER,* VOL. 37, PP. 223-232, 2010.

[6] A. ÜNDAR, *ET AL.*, "EFFECTS OF PULSATILE AND NONPULSATILE PERFUSION ON CEREBRAL HEMODYNAMICS INVESTIGATED WITH A NEW PEDIATRIC PUMP.," *THE JOURNAL OF THORACIC AND CARDIOVASCULAR SURGERY,* VOL. 124, PP. 413-416, 2002.

[7] D. L. ECKBERG, "BAROREFLEX INHIBITION OF THE HUMAN SINUS NODE: IMPORTANCE OF STIMULUS INTENSITY, DURATION, AND RATE OF PRESSURE CHANGE," *THE JOURNAL OF PHYSIOLOGY,* VOL. 269, PP. 561-577, 1977.

[8] K. G. SOUCY, *ET AL.*, "DEFINING PULSATILITY DURING CONTINUOUS-FLOW VENTRICULAR ASSIST DEVICE SUPPORT," *THE JOURNAL OF HEART AND LUNG TRANSPLANTATION,* VOL. 32, PP. 581-587, 2013.

[9] B. P. MEYNS, *ET AL.*, "CLINICAL BENEFITS OF PARTIAL CIRCULATORY SUPPORT IN NEW YORK HEART ASSOCIATION CLASS IIIB AND EARLY CLASS IV PATIENTS," *EUR J CARDIOTHORAC SURG,* VOL. IN PRESS, CORRECTED PROOF, 2011.

[10] G. WRIGHT, "MECHANICAL SIMULATION OF CARDIAC FUNCTION BY MEANS OF PULSATILE BLOOD PUMPS.," *JOURNAL OF CARDIOTHORACIC AND VASCULAR ANESTHESIA,* VOL. 11, PP. 299-309, 1997.

[11] A. ÜNDAR, *ET AL.*, "QUANTIFICATION OF PERFUSION MODES IN TERMS OF SURPLUS HEMODYNAMIC ENERGY LEVELS IN A SIMULATED PEDIATRIC CPB MODEL," *ASAIO JOURNAL,* VOL. 52, PP. 712-717, 2006.

[12] T. NISHINAKA, *ET AL.*, "EFFECTS OF REDUCED PULSE PRESSURE TO THE CEREBRAL METABOLISM DURING PROLONGED NONPULSATILE LEFT HEART BYPASS," *ARTIFICIAL ORGANS,* VOL. 24, PP. 676-679, 2000.

[13] K. BOURQUE, *ET AL.*, "IN VIVO ASSESSMENT OF A ROTARY LEFT VENTRICULAR ASSIST DEVICE-INDUCED ARTIFICIAL PULSE IN THE PROXIMAL AND DISTAL AORTA," *ARTIFICIAL ORGANS,* VOL. 30, PP. 638-642, 2006.

[14] R. B. SHEPARD, *ET AL.*, "ENERGY EQUIVALENT PRESSURE," *ARCHIVE OF SURGERY,* VOL. 93, PP. 730-740, 1966.

[15] D. TIMMS, *ET AL.*, "BIVACOR® - A MAGNETICALLY LEVITATED BIVENTRICULAR ARTIFICIAL HEART," IN *PROCEEDINGS OF THE 20TH MAGDA CONFERENCE IN PACIFIC ASIA* KAOHSIUNG, TAIWAN, 2011, PP. 482-487.

[16] J. PYRHONEN, *ET AL.*, *DESIGN OF ROTATING ELECTRICAL MACHINES*: JOHN WILEY & SONS, 2008.

[17] J. GU, *ET AL.*, "DRIVING AND BRAKING CONTROL OF PM SYNCHRONOUS MOTOR BASED ON LOW-RESOLUTION HALL SENSOR FOR BATTERY ELECTRIC VEHICLE," *CHINESE JOURNAL OF MECHANICAL ENGINEERING,* VOL. 26, PP. 1-10, 2013.